Sponge Mesoporous Silica Formation Using Disordered Phospholipid Bilayers as Template

Anne Galarneau,*,† Federica Sartori,†,‡,§ Michela Cangiotti,‡,§ Tzonka Mineva,†,§ Francesco Di Renzo,†,§ and M. Francesca Ottaviani*,‡

Institut Charles Gerhardt Montpellier, UMR 5253 CNRS/UM2/ENSCM /UM1, ENSCM, 8 rue de l'Ecole Normale, 34296 Montpellier Cedex 5, France, and Department of Geological Sciences, Chemical and Environmental Technologies, University of Urbino, Loc. Crocicchia, 61029 Urbino, Italy

Received: September 12, 2009; Revised Manuscript Received: January 8, 2010

Lecithin/dodecylamine/lactose mixtures in ethanol/aqueous media led to the formation of sponge mesoporous silica (SMS) materials by means of tetraethoxysilane (TEOS) as silica source. SMS materials show a "sponge-mesoporous" porosity with a pore diameter of about 5−6 nm, in accordance to the length of a lecithin bilayer. SMS synthesis was developed to create a new class of powerful biocatalysts able to efficiently encapsulate enzymes by adding a porosity control to the classical sol−gel synthesis and by using phospholipids and lactose as protecting agents for the enzymes. In the present study, the formation of SMS was investigated by using electron paramagnetic resonance (EPR) probes inserted inside phospholipid bilayers. The influence of progressive addition of each component (ethanol, dodecylamine, lactose, TEOS) on phospholipid bilayers was first examined; then, the time evolution of EPR spectra during SMS synthesis was studied. Parameters informative of mobility, structure, order, and polarity around the probes were extracted by computer analysis of the EPR line shape. The results were discussed on the basis of solids characterization by X-ray diffraction, nitrogen isotherm, transmission electron microscopy, and scanning electron microscopy. The results, together with the well-known ability of ethanol to promote membrane hemifusion, suggested that the templating structure is a bicontinuous phospholipid bilayer phase, shaped as a gyroid, resulting of multiple membrane hemifusions induced by the high alcohol content used in SMS synthesis. SMS synthesis was compared to hexagonal mesoporous silica (HMS) synthesis accomplished by adding TEOS to a dodecylamine/EtOH/water mixture. EPR evidenced the difference between HMS and SMS synthesis; the latter uses an already organized but slowly growing mesophase of phospholipids, never observed before, whereas the former shows a progressive elongation of micelles into wormlike structures. SMS-type materials represent a new class of biocompatible materials and open a bright perspective for biomolecule processing for pharmaceutical, biocatalysis, biosensors, or biofuel cell applications.

Introduction

The first successful preparation of mesoporous micelle-templated silica (MTS) materials was achieved using cetyltrimethyl ammonium bromide (CTAB) surfactants and tetraethoxysilane (TEOS) in ammoniac solution in 1971 by Sylvania Electric Products, Inc.[1] giving a hexagonal structure, presented as low density silica. The properties of MTS were then disclosed in 1991 by Mobil Oil Company[2] and named MCM-41 for the hexagonal structure. MTS family was then rapidly extended to different hexagonal and cubic structures. Silica sources (lamellar silica, fumed silicas, sodium silicates, organo alkoxysilanes, and so forth) have been varied as well as the surfactant type (alkyl quaternary ammonium, alkyl amine, tribloc copolymers, alkyl oligomers), the conditions of reactions (acidic, basic, neutral with NaF addition, and so forth), the temperature and the use of cosurfactants (trimethylbenzene, decane, butanol, etc.) giving rise to an extended family of MTS with different symmetries and names (MCM-41, MCM-48, HMS, SBA-15, SBA-16, MCF, MSU-x, KIT-6, etc.).[3] To date silica remains the most studied material and promising results have been obtained in the field of chromatography, catalysis, and more recently for applications as biomaterials in biocatalysis or biosensors[4−6] and biomedical devices as drug delivery.[7] More than 150 publications are related to proteins or enzymes immobilization in MTS materials. Mostly, enzyme immobilization is performed by adsorption in calcined mesoporous materials (see for examples the review in ref 5). Also, in silica sol−gel encapsulation, enzymes[8] or bacteria[9−11] have been successfully immobilized and are biologically active, owing to additives such as sugars, glycerol, charged polymers (poly-vinylimidazole, -ethyleneimine, -ethyleneglycol) or gelatin. Additives help to stabilize proteins against the denaturing stresses encountered upon sol−gel entrapment. Successful studies have been performed by sol−gel methods, for lipases encapsulation,[12,13] by using poly(vinyl alcohol), but the diffusivity of the substrates are limited due to the uncontrolled porosity.

Recently, we have developed a new class of mesoporous silica material, referred to "sponge mesoporous silica" (SMS), synthesized using lecithin/dodecylamine/lactose as templates in an ethanol/aqueous media.[14−16] In the presence of lipase during the synthesis, the lipase-SMS exhibited higher catalytic activity, compared to traditional sol−gel procedure or postsynthesis immobilization in MTS. It was demonstrated that lactose was

* To whom correspondence should be addressed. (A.G.) Tel.: +33 467163468. Fax: +33 467163470. E-mail: anne.galarneau@enscm.fr (M.F.O.) Tel. +390722304320. Fax: +390722304240. E-mail: maria.ottaviani@uniurb.it.

† Institut Charles Gerhardt Montpellier.

‡ University of Urbino.

§ E-mail addresses: (F.S.) federica_sartori@virgilio.it; (M.C.) michela.cangiotti@uniurb.it; (T.M.) tzonka.mineva@enscm.fr; (F.D.R.) francesco.di-renzo@enscm.fr.

10.1021/jp908828q
Published on Web 01/28/2010

the most efficient sugar to preserve enzyme-SMS activity. The high catalytic activity was explained by the use of lecithin/dodecylamine assembly structure permitting easy diffusion of substrates, through the generation of 3D mesoporosity in silica sol−gel, and also to the use of natural and biocompatible surfactants. Indeed, classical trimethylalkylammonium surfactants like cetyltrimethylammonium bromide (CTAB) used in MCM-41 synthesis are inhibitors for the enzymes. Lecithin is a trivial name for zwitterionic 1,2-diacyl-*sn*-3-phosphatidylcholine. It belongs to the phospholipids family, which forms the lipid matrix of biological membranes. As a biocompatible surfactant, it is widely used in every day life, including human and animal food, medicine, cosmetics, and manifold industrial applications.[17] Because of its nearly cylindrical molecular shape, lecithin cannot grow micelles by itself in aqueous media. Its tendency to curve, described in terms of its spontaneous curvature, is very low, and therefore it induces the formation of bilayer phospholipids structures, lamellar structures, described as membranes, vesicles, or liposomes. Lecithin contains residues of phosphatocholine, glycerol, and two fatty acids, but commercial lecithin also contains residues of different phospholipids, depending on the origin and purification grade.

The effect of the addition of ethanol into biological membranes in aqueous solution is a subject of debate and controversy. The ability of ethanol to enhance membrane permeability[18] is exploited in transdermal drug delivery, where ethanol is a common component of topical formulations. However high concentrations of ethanol can delay drug penetration.[19] Numerous experimental and computational studies have been focused on the interaction of ethanol with lipid membranes. A very recent study of structure simulation concerning the interaction of ethanol with phospholipid bilayers helps to understand the effect of ethanol on bilayer structures as a function of the ethanol content.[20] Although ethanol has an amphiphilic character, being a short-chain alcohol, its hydrophobicity is limited. Therefore at low content of ethanol (<30% in volume), the ethanol molecules are at the lipid/water interface just beneath the phosphate groups of the lipids suggesting a strong interaction (hydrogen-bond) between lipid head groups and ethanol molecules. No ethanol is found neither in the hydrophobic core of the bilayer nor in the water phase. This statement is in accordance with 2D-NMR results, where ethanol molecules have been localized near the glycerol backbone, upper methylene segments of lipid hydrocarbon chains.[21] Furthermore, the addition of ethanol gives rise to an increase in the area of the phospholipid head groups, leading to (i) disordering of the lipid acyl chains, (ii) diminution of the bilayer thickness, and (iii) increase of membrane fluidity responsible of enhanced permeability. At high ethanol content (>30% in volume), ethanol molecules penetrate into the hydrophobic core of the bilayer increasing the hydrophilicity of the membrane interior. A wave motion of the lipid bilayer creates positive and negative curvature in the membrane. This permits water penetration in the membrane interior as well as migration of phospholipids inside the bilayer giving rise to clusters of water molecules surrounded by phospholipid head groups (shaped as inversed micelles). The simulation shows that ethanol supports a negative curvature of the membrane, as emerging stalk during membrane hemifusion. The resulting 3-dimensional membrane structure may serve as starting templates for solid material synthesis.[21] The formation of micelle-like structures is in line with laboratory experiments that have revealed that the bilayer structure in a DPPC lipid system is lost at ethanol content higher than 30% in volume and the formation of globular structures is observed.[22]

In this study, the SMS synthesis was performed by using an ethanol content of 48% in volume; this percentage is expected to form thinner and weaker phospholipids bilayer structures. The synthesis gives rise to a 3D porous network. Therefore, the templating structure may arise from the formation of either undulations in the bilayer creating a 3D structure that silica stabilizes, or micelles, which self-assemble with silica to evolve toward a 3D structure upon silica condensation, as it has already been observed by in situ EPR for other mesoporous silica (MCM-41,[23−29] SBA-15,[30,31] and KIT-6[32]).

The formation of SMS material was investigated by means of the electron paramagnetic resonance (EPR) technique by using the same EPR probes already used for MCM-41 synthesis,[23−29] that is, 4-cetyldimethyl ammonium-2,2,6,6-tetramethyl-piperidine-N-oxide bromide (CAT16) and 5-doxyl stearic acid (5DSA). The computer aided analysis of the EPR line shape indicated that these probes are inserted inside phospholipid bilayers. The modifications of the phospholipid bilayers generated by progressive addition of each component in the SMS synthesis (in sequence, ethanol, lactose, dodecylamine, and TEOS) were first studied in water solution by EPR, and then the evolution of the EPR spectra during the SMS material formation was followed within time and compared to the characterization results obtained for the solids at different synthesis time by X-ray diffraction (XRD), nitrogen isotherm, scanning electron microscope (SEM), and transmission electron microscopy (TEM). SMS synthesis was compared to the synthesis of hexagonal mesoporous silica (HMS) materials.[33−35] The HMS synthesis was performed by using dodecylamine/EtOH/water and TEOS, featuring a worm-like structure, corresponding to a disordered hexagonal structure with interconnections between wormlike channels.[36] This study is therefore aimed to investigate SMS materials, as a new class of biocompatible materials, for pharmaceutical, biocatalysis, biosensors, or biofuel cell applications, but it also helps to understand the effect of ethanol on phospholipid bilayer membranes, discussing the results on the basis of the hypothetic structures predicted by simulation. Finally, the comparison between SMS and HMS synthesis clarifies the role of phospholipids in modifying structures and kinetics of formation of the solids.

Experimental Section

Materials. SMS materials synthesis using lecithin have been performed using TEOS from Aldrich, lecithin from egg yolk (L-α Lecithin) (Fluka), and β-D-lactose (Aldrich). Egg yolk lecithin is a natural and low cost phospholipid. It consists of a mixture of phospholipids with different chain lengths and insaturations on the fatty acyl chain. The acylchains will be noted C *n*:*m* where *n* is the number of carbon atoms of the chain and *m* the number of insaturations in the chain. Egg yolk lecithin is composed of 1.8% myristic acid (C14:0), 36.5% palmitic acid (C16:0), 14% stearic acid (C18:0), 4.3% palmitoleic acid (C16:1), 30% oleic acid (C18:1), 13.5% linoleic acid (C18:2). The same lecithin batch was used for all analysis, but reproducibility was controlled by using different batches. Dodecylamine (DDA) from Aldrich has been used as coadditive in SMS synthesis and as surfactant in the HMS materials synthesis. EPR probes were 4-cetyldimethylammonium-2,2,6,6-tetramethyl-piperidine-*N*-oxide bromide (CAT16, kindly provided by Dr. Xuegong Lei, Columbia University, New York) and 5-doxylstearic acid (5DSA, Aldrich).

Synthesis of SMS Material. SMS was prepared as previously described,[14−16,36] using the molar ratios 1 TEOS/0.11 lecithin/0.084 dodecylamine/0.068 lactose/56 H_2O/17 ethanol. A first

solution of lactose and water was prepared and added slowly under stirring to a second solution containing lecithin and dodecylamine in ethanol, until a homogeneous emulsion was formed. TEOS was then added slowly under stirring for 15 min, and the mixture was left for 24 h in static conditions at 37 °C. The slurry was then centrifuged and washed 5 times with a ethanol/water mixture (1/1, v/v) followed by centrifugation. The samples were then dried for 16 h at 50 °C. The calcination of the resulting materials was performed under air flow at 550 °C for 8 h.

Synthesis of HMS Material. The HMS material was synthesized using DDA as templating surfactant in water−ethanol solution and then adding TEOS at molar ratios 1 TEOS/0.25 Dodecylamine/7.12 EtOH/36 H_2O with the following procedure: dodecylamine was dissolved in ethanol and water under stirring, then TEOS was slowly added. The mixture was stirred in a close container for 1 h at 25 °C and then in static for 24 h at 25 °C. The slurry was then filtered and dried unwashed at 80 °C overnight. The calcination of the resulting material was performed under air flow at 550 °C for 8 h. This HMS material contains 3% water, 52% dodecylamine (half protonated), and 46% silica.

EPR Analysis. The synthesis mixtures described above were reprepared by adding the EPR probes, CAT16 or 5DSA. The spin probes were added to phospholipid aggregates (for SMS synthesis) or to DDA aggregates (for HMS synthesis) in water solution with a molar ratio of 1 radical/1000 phospholipid (or DDA) and left equilibrating for 1 day before being used in the synthesis. Fifty microliters of the slurry was put in an EPR tube (2 mm i.d.) just after 14 min stirring with TEOS, and the tube was inserted in the EPR cavity at 37 °C. The tuning of the EPR cavity and temperature equilibration took 1 min. The kinetics of the syntheses were followed over time thanks to EPR spectra taken every 5 min. EPR spectra at 37 °C were also recorded for reference samples obtained by subsequent addition of each component used in the SMS synthesis in the following order: probe, water, phospholipid, ethanol, lactose, dodecylamine, and TEOS. Similarly, for the HMS synthesis the reference samples were obtained by adding the components in the following order: probe, water, dodecylamine, ethanol, and TEOS.

Computer-Aided Analysis of the EPR Spectra. The spectra were computed by means of the well-established procedure by Budil and Freed.[37,38] The computation allowed us to extract the following main magnetic and mobility parameters: (a) the g_{ii} main components of the tensor for the coupling between the electron spin and the magnetic field (where not differently specified, these parameters were assumed 2.009, 2.006, 2.003, as already used for previous studies with the same probes); (b) the A_{ii} main components of the tensor for the coupling between the unpaired electron spin and the nuclear nitrogen spin ($I_N = 1$) (the increase of these components corresponds to an increase in the environmental polarity of the probes). Where not differently specified, $A_{xx} = A_{yy} = 7$ G was assumed for CAT16 and $A_{xx} = A_{yy} = 6$ G for 5DSA, and the parameter which reports on the polarity variation is A_{zz}, or, for a better comparison, $\langle A_N \rangle = (A_{xx} + A_{yy} + A_{zz})/3$. The accuracy in the A_{ii} parameters is ±0.01 G but it decreases for broadened spectra; (c) the correlation time for the rotational motion, τ (the increase of this parameter monitors an increased interaction strength of the probe with its environment; unless otherwise specified, we assumed a Brownian rotational diffusional motion, with $\tau = 1/(6D)$, where D is the diffusion coefficient). Because of the diffusional model and probe geometry, the main mobility parameter is the perpendicular component of the correlation time, that is, τ_{perp}. The main rotation of the probes around the N−O direction, corresponding to the chain direction, leads to calculation independence on variations of the parallel component. In line with this finding, also a tilt angle of the rotational axis was not included in the calculation. The accuracy in τ_{perp} is ±0.01 ns but it decreases for broadened spectra; (d) the order parameter, S, which changes from 0 (no order) to 1 (maximum order). This parameter is introduced in the computation (in form of the $C_{2,0}$ coefficient in the correspondent Hamiltonian component) in the case of 5DSA probe, when the nitroxide group at position 5 of the carbon chain is positioned in the well packed chain area of a lipid monolayer and it monitors the order of the chains themselves. The accuracy in the order parameter is ±0.01.

If the spectra are constituted by different signals arising from not exchangeable probes (in the EPR time scale), these signals superimpose each other to generate the overall EPR spectrum. Subtraction of spectra containing the signals at different relative intensities allows us to extract the signals themselves and to compute each of them. The subtraction procedure also provides the percentages of the signals (accuracy ±0.01%).

Instrumentation. Powder X-ray diffraction (XRD) patterns were recorded on a Bruker AXS D8 diffractometer by using CuKα radiation and Ni filter. The adsorption−desorption isotherms for nitrogen at 77 K were measured using a Micromeritics ASAP 2010 instrument on samples previously calcined at 550 °C in air for 8 h. Average pore diameters have been evaluated from the nitrogen desorption branch according to Broekhoff and de Boer (BdB) method,[39] this method being the one leading to the best evaluation of pore size for mesostructured materials.[40] Examination of the particles morphology was achieved using a Hitachi S-4500 I SEM. TEM was performed on a JEOL 1200 EX II microscope operating at 120 keV. The particles were trapped in a resin (LR White) and cut into slices 70 nm thick by ultramicrotomy before to be imaged. The EPR spectra were recorded by means of a EMX-Bruker spectrometer operating at X band (9.5 GHz) and interfaced to a IBM PC computer (Bruker software) for data acquisition and handling. The temperature was controlled with a Bruker ST3000 variable-temperature assembly. The spectra were considered valid only on condition of reproducibility of the spectral line shape for different samples of the same materials in the same experimental conditions.

Results and Discussion

EPR Studies of Phospholipids Bilayer Evolution (In Solution) by Progressive Addition of SMS Synthesis Reactants Using CAT16 As Probe. Before analyzing, by EPR, the modifications of the SMS synthesis mixtures over time, it is necessary to understand how each reactant (lecithin, ethanol, lactose, dodecylamine, and TEOS) used in SMS synthesis is able to change the EPR signal due to structural and mobility modifications of the spin probe environment. The experimental and computed EPR spectra of CAT16, obtained for the "blank" samples, starting from pure lecithin in water and then progressively adding the other additives needed for the SMS synthesis, are reported in Figure S1 (in Supporting Information). The main parameters used for the computations are listed in Table 1.

On the basis of parameter variations, the following information were extracted:

(1) In the absence of ethanol, CAT16 chain inserts in the packed phospholipids chains, while the probe head inserts among phospholipid heads. The mobility of the probe decreased from water ($\tau_{perp} = 0.19$ ns) to the bilayer ($\tau_{perp} = 3.14$ ns), while the polarity increased ($\langle A_N \rangle = 15.88$ G in water; $\langle A_N \rangle$

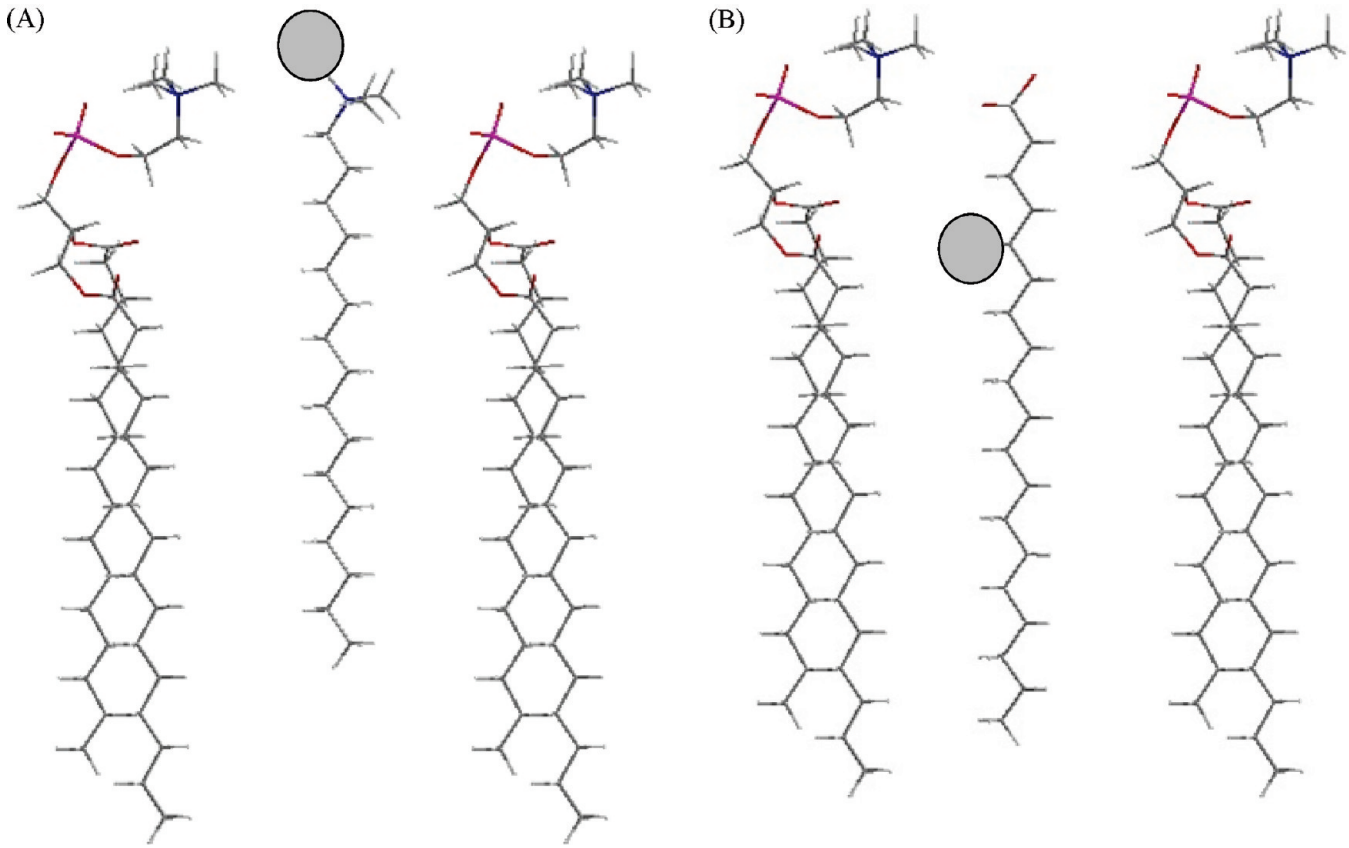

Figure 1. Schematic location of (A) CAT16 and (B) 5DSA probes into phospholipid membrane in a water/ethanol medium. Nitroxide moieties are represented by gray circles.

TABLE 1: Main Parameters Used for the Computation of CAT16 EPR Spectra (Lec = lecithin, W = water, EtOH = Ethanol, Lac = β-lactose, DDA = dodecylamine)*

samples - CAT16	$\langle A_N \rangle$/G (polarity)	%	τ_{perp}/ns (interaction)
W	15.88	100	0.19
Lec−W	16.00	100	3.14
Lec−W−EtOH	16.05	100	1.10
Lec−W−EtOH−Lac	16.03	95	2.20
Lec−W−EtOH−Lac−DDA	16.08	80	1.30
	16.11	20	0.19
Lec−W−EtOH−Lac−DDA−TEOS (begin SMS synthesis)	15.87	90	2.76
	16.17	10	12.5
DDA−W	16.67	90	0.66
	Not meas (broad)	10	Not meas (broad)
DDA−W−EtOH	16.08	100	0.49
DDA−W−EtOH−TEOS (begin HMS synthesis)	16.5	93	17.0
	16.3	7	0.55

* The g_{ii} components were assumed constant (g_{ii} = 2.009, 2.006, 2.003) and we also assumed $A_{xx} = A_{yy}$= 7 G. $\langle A_N \rangle$ was calculated as ($A_{xx} + A_{yy} + A_{zz}$)/3. The accuracy of the percent is 1%; the accuracy of $\langle A_N \rangle$ and τ_{perp} is ±0.01.

= 16.00 G in bilayer). The increase in polarity is because of location of the nitroxide group close to the charged (zwitterionic) lecithin head. While the cetyl chain of CAT16 inserts among the lecithin hydrophobic chains, the positively charged CAT16 head is attracted by the negatively charged phosphate group. The decrease in mobility is therefore because of the insertion of CAT16 inside the rigid lecithin bilayer. Figure 1a and Figure 2 (first picture) schematically depicts the location of CAT16 in the phospholipid aggregate.

(2) In the presence of ethanol, CAT16 probe monitors a decreased packing of the phospholipid bilayer. The addition of ethanol is described in Figure 2 for simplicity as a gray area in the region just below the phospholipid heads. At a volume ratio of 48% (EtOH/water) EtOH leads to an increase in mobility of CAT16 (τ_{perp} = 3.14 ns, in bilayer; τ_{perp} = 1.10 ns, in bilayer + EtOH) and in polarity ($\langle A_N \rangle$ = 16.00 G, in bilayer; $\langle A_N \rangle$ = 16.05 G, in bilayer + EtOH). As calculated by simulation study,[20] ethanol induces a separation between phospholipids heads up to 70%. The area per lecithin is known to be equal to 85 Å^2.[41] Hence, an increase of 70% results in an area per lecithin of 144 Å^2. This enhanced space between phospholipids allows the probe to lose interaction with lecithin and, consequently, to increase its mobility. However, the increase in polarity of CAT16, even small, indicates that the CAT16 head is slightly shifted toward the charged zwitterionic group (Figure 2) at the water/membrane interface, due to the decreased rigidity of the phospholipid bilayer.

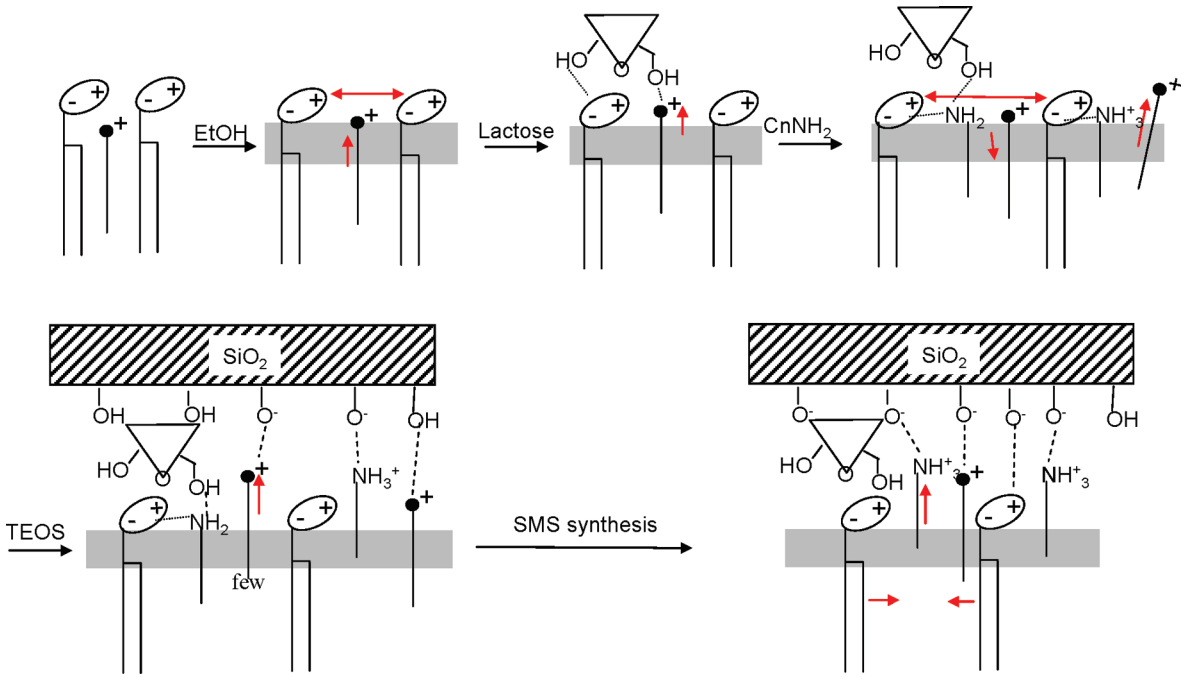

Figure 2. Schematic evolution of the phospholipid bilayer system and CAT16 as a function of progressive addition of SMS reactants. Molecular movements are represented by red arrows. In summary, ethanol works as phospholipid-spacer; β-lactose interacts (by hydrogen-bondings) with the lipid heads; DDA, inserting in the bilayer, impedes lactose-CAT16 hydrogen-bonding; a poorly structured solid is formed at the beginning of SMS synthesis, which progressively transforms into well-structured SMS due to protonation and consequent electrostatic interactions of DDA amino groups.

(3) In the presence of ethanol, lactose interacts (by hydrogen bonding) with the charged lipid heads at the membrane/solution interphase. The addition of lactose leads to an unpredicted perturbation of the freedom gained by ethanol addition; the mobility and the polarity of CAT16 both decreased ($\tau_{perp} = 1.10$ ns and $\langle A_N \rangle = 16.05$ G, in bilayer + EtOH; $\tau_{perp} = 2.20$ ns, and $\langle A_N \rangle = 16.03$ G, in bilayer + EtOH + lactose). Lactose is soluble in water and has poor affinity for ethanol. Therefore, lactose is supposed to be located in the water region at the surface of the lipid membrane (Figure 2), and it should theoretically have a negligible effect on the membrane structure. However, from EPR results we observe that lactose interacts with CAT16, thus decreasing the freedom of the nitroxide group, very probably through hydrogen bonding between lactose-OH and CAT16-quaternary ammonium (Figure 2). Likely, such interaction also occurs between lactose and the phospholipid head. However, it is noticeable that the effect of lactose is driven by ethanol, since the addition of lactose to the ethanol-free phospholipid bilayer (in water only) does not produce any effect (results not shown). This is because, as indicated at point (2), ethanol induces a separation between the phospholipid heads, allowing the CAT16 heads to merge at the surface of the membrane and consequently permitting the occurrence of CAT16-lactose hydrogen bonding.

(4) Dodecylamine, added to the water/lecithin/ethanol/lactose mixture, inserts in the lecithin bilayer and interacts with CAT16 (head-to-head), but a 20% probe-fraction is removed from the bilayer. The EPR results show that DDA almost annuls the effect of lactose described at point (3) and separates the probes into two environments. Indeed, 80% of the probes shows mobility and polarity conditions ($\tau_{perp} = 1.30$ ns and $\langle A_N \rangle = 16.08$ G) similar to those found for the solution of lecithin in water/ethanol at point (2) ($\tau_{perp} = 1.10$ ns and $\langle A_N \rangle = 16.05$ G). In the meantime, 20% of the probes is expulsed from the bilayer to the interface, since these probes show the same mobility ($\tau_{perp} = 0.19$ ns) as the probes in water, but the polarity ($\langle A_N \rangle = 16.11$ G) increases because of the presence of phospholipid-charged groups around the nitroxide. Therefore, DDA head locates at the water/membrane interface and replaces the CAT16/lactose interaction by a stronger amine/lactose interaction (Figure 2). Consequently, CAT16 is no more interacting with lactose and recovers its mobility. Eighty percent of the probes shows the same conditions as in water/ethanol solution with an improved interaction with phosphate groups (as tested by the slight increase in τ_{perp} and $\langle A_N \rangle$). Fatty amines are known to increase the area per lecithin from 85 to 140 Å^2 and to increase interfacial tension of phospholipids membrane, by forming a phospholipid/fatty amine = 1:1 complex in the membrane through $-NH_3^+$—P$-$O$^-$ electrostatic bonds.[41] The increase of area per lecithin due to fatty amines is in the same range as the one due to EtOH addition; so DDA probably inserts inside phospholipids without changing the space between phospholipid heads and accounts for the similar behavior of CAT16 in lecithin/ethanol/water solution and in lecithin/ethanol/water/lactose/DDA solution. Petelska et al. reports the formation of fatty-amine/lecithin complexes inside lecithin membrane at fatty-amine/lecithin molar ratio <0.6;[41] for fatty-amine amounts ≥ 0.6, the solutions granulate indicating that the bilayer is destroyed. In the present case of the SMS synthesis mixture, the DDA/lecithin molar ratio is 0.3, which leads to a phospholipid/DDA = 1:1 complex. Moreover, SMS synthesis is successfully performed for molar ratios as high as 0.5, giving rise to an increase of both surface area and pore volume due to the catalytic effect of the amine on the silica condensation. However, such a high DDA content lowers the biocatalytic activity.[36] The final SMS material (after washing and drying) is characterized by 1 Lecithin/0.4 DDA/0.3 lactose molar ratio. Therefore, half of the space between phospholipid heads is occupied by an alkylamine,[36] and almost each DDA interacts with a lactose molecule by hydrogen bonding, giving rise to NH_2 and NH_3^+ heads interacting with both OH lactose groups and P$-$O$^-$ phospholipid groups (Figure 2).

5. After TEOS addition to the water/lecithin/ethanol/lactose/DDA mixture (15 min equilibration), a poorly structured solid is formed. The addition of TEOS and 15 min equilibration represent the starting point of the SMS synthesis. After this equilibration, 10% of CAT16 shows a spectral component characteristic of probes electrostatically interacting with silicates of an already structured solid surface (Figure 2) at low mobility (τ_{perp} = 12.5 ns) and at quite high polarity ($<A_N>$ = 16.17 G). Interestingly, most of the probes (90%) also shows slow motion conditions (τ_{perp} = 2.76 ns), and a polarity ($<A_N>$ = 15.87 G) a little bit lower than the polarity of CAT16 in water. This means that 90% of the probes is interacting with silanols from a partly polymerized silica (Figure 2), which transforms into an organized solid structure in the following synthesis time (see below in the section about the kinetics). We may depict the system as follow: TEOS penetrates into the water network at a disordered membrane surface by progressive hydrolysis of Si−OEt bonds to form Si−OH. Hydrated silanols induce a lower polarity around the probes, but then SiOH progressively deprotonates to form Si−O^-. The relatively weak CAT16/silanol interaction progressively transforms into a stronger electrostatic interaction ammonium/silicate. When silicates are formed, Si−O^- groups electrostatically interact with ammonium head groups from (i) phospholipids; (b) DDA; and (c) CAT16 (Figure 2). Also, at the beginning of the synthesis dodecylamine interacts with lactose at the water interface and so is prevented from interacting with silanols. Therefore, DDA cannot act as a catalyst for silanol hydrolysis, deprotonation, and silica condensation. The dodecylamine/lactose interaction is progressively substituted by a dodecylamine/SiOH interaction, leading to dodecylammonium/SiO^- interaction. This interaction exchange controls the kinetics of condensation of silica. As presented below, the kinetics of SMS formation is slow, because silanol deprotonation is slow due to the competing interaction of dodecylamine with lactose. Albeit this exchange, lactose remains trapped into the solid structure by interacting with phospholipid heads and prevents a direct inauspicious interaction of silica with enzymes embedded in the phospholipid bilayer.

EPR Studies of Dodecylamine (DDA) Aggregate Evolution (In Solution) by Progressive Addition of SMS Synthesis Reactants Using CAT16 As Probe. SMS synthesis was compared to HMS synthesis, accomplished by adding DDA, EtOH, and TEOS in water solution.[33−35] HMS synthesis serves as reference system to clarify the role of phospholipids in SMS synthesis. First, the effect of the progressive addition of each component of the HMS synthesis to the CAT16−water solution was examined by EPR (Figure S2 in Supporting Information).

- CAT16 probe inserts into DDA liquid crystal aggregates in water. This information stem from the following results: From water (τ_{perp} = 0.19 ns; $<A_N>$ = 15.88 G) to DDA/water solutions (τ_{perp} = 0.66 ns; $<A_N>$ = 16.17 G), CAT16 mobility decreases while CAT16 polarity increases. These variations indicate that the probe inserts into DDA aggregates. It is noticeable that CAT16 presents a higher motion and polarity in DDA aggregates in comparison to phospholipid bilayer, showing that the DDA aggregates are more fluid than the phospholipid bilayer. When embedded in DDA aggregates, CAT16 head is in direct contact with the water interphase, which is not the case for CAT16 in the phospholipid system. From literature it is known that DDA does not form micelles, but liquid nematic crystals.[44] In this context, the CAT16 chain is inserted into a fluid DDA chain aggregate and the NO group is in vicinity of the protonated and/or hydrated amino groups of DDA, feeling a significant increase in environmental polarity.

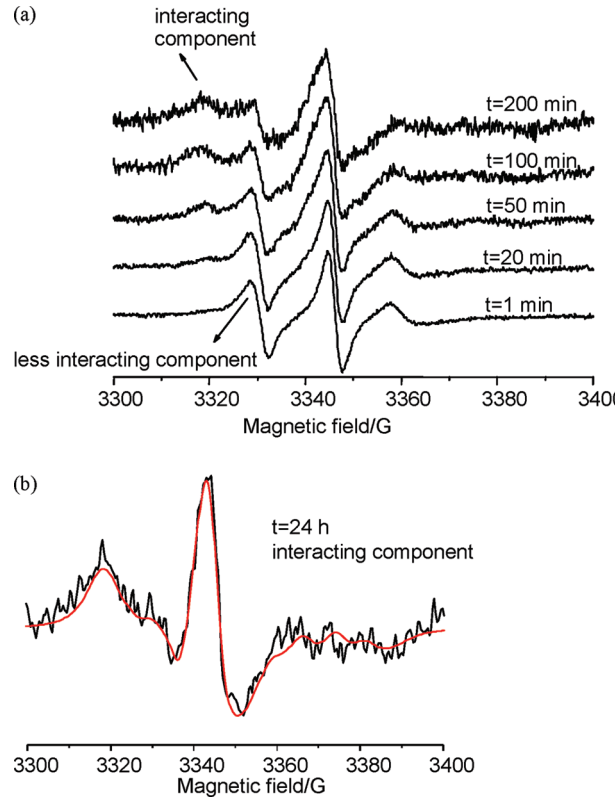

Figure 3. (a) Examples of EPR spectra (T = 310 K, magnetic field range: 3300−3400 G) for CAT16 at different SMS synthesis times (lecithin/water/ethanol/lactose/dodecylamine + TEOS). The low field peaks of the interacting and less interacting components are indicated by arrows. (b) Computation of the interacting component (experimental subtracted spectrum at 310 K, black line; computed signal, red line) of CAT16 obtained after one day of SMS synthesis.

- CAT16 probe shows the fluidification effect of ethanol in the DDA/water/ethanol mixture. Indeed, the addition of EtOH to the DDA−water system leads to an increase in mobility (τ_{perp} = 0.49 ns) and a decrease in polarity ($<A_N>$ = 16.08 G); ethanol is disturbing DDA aggregates inserting itself among the amino heads and increasing the area per amino head. Consequently, the nitroxide environment is modified from water into a less polar water/EtOH medium, while the electrostatic interactions between CAT16 and DDA heads diminish. Caldararu et al.[45] describe this system as a microemulsion. The mixture for HMS synthesis before TEOS addition is therefore a fluid homogeneous system.

- The HMS organized structure is already formed after 15 min equilibration of a DDA/water/ethanol/TEOS mixture. After TEOS addition, the spectrum obtained after 15 min equilibration represents the starting point of the HMS synthesis, but already shows a remarkable decrease in mobility (τ_{perp} = 17 ns) and an increase in polarity ($<A_N>$ = 16.50 G), revealing an electrostatic interaction of the probe with the silicates from the beginning of the synthesis. Also, DDA heads are expected to strongly interact, by hydrogen bonding and electrostatic interactions (as such as NH_2—HO−Si and NH_3^+—$^-$O−Si bonds, respectively), with the silica surface already formed after 15 min of reaction. This is due to the nucleophilic interaction between amino group and silica that promotes silica condensation, quicker than in the case of SMS, where amino groups are also interacting with lactose. The spectrum does not change overtime (see below in the section about the kinetics); this means that the HMS surface does not change over time, contrary to the SMS synthesis.

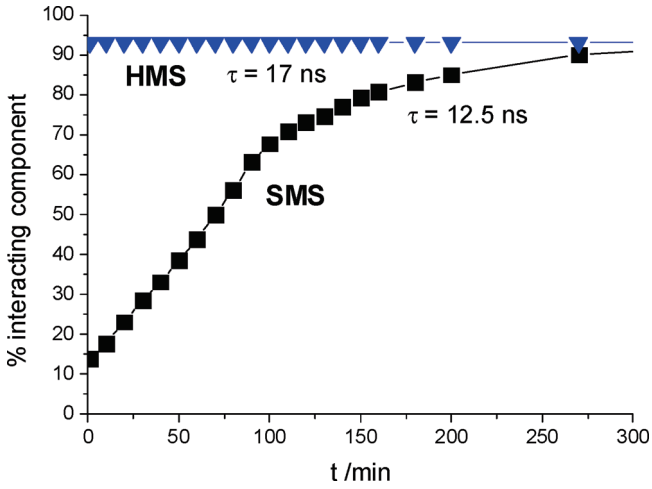

Figure 4. Percentage of interacting component for CAT16 probe as a function of time (0−300 min) for SMS and HMS syntheses.

Kinetics of SMS and HMS Synthesis by Means of CAT16 Probe. As discussed above, the HMS (DDA + water + ethanol + TEOS) synthesis is already finished at $t = 0$, that is, after 15 min of mixture equilibration. Even after 2 days the spectrum is the same as the one shown at the bottom of Figure S2 (in Supporting Information). On the opposite, for the SMS synthesis the EPR line shape changes over time. Figure 3a shows some indicative EPR spectra at different times for the SMS synthesis (lecithin + DDA + lactose + ethanol + water + TEOS). As discussed in a previous section, the beginning condition at $t =$ 0 min already shows a fraction (10%) of the so-called interacting component. The other component (termed less interacting) at the beginning of SMS synthesis progressively transforms into the interacting one, up to a relative percentage of 90% after 5 h synthesis. Longer synthesis times (24 h) do not affect the spectrum. Figure 3b shows the computation of the interacting component. It is interesting to compare the main computation parameters of the interacting components for SMS and HMS

Interacting component SMS: $A_{ii} = 7.5, 5.0, 36.0$ G; $\langle A_N \rangle =$ 16.17 G; $\tau_{perp} = 12.5$ ns.

Interacting component HMS: $A_{ii} = 8.0, 5.0, 36.5$ G; $\langle A_N \rangle =$ 16.50 G; $\tau_{perp} = 17.0$ ns.

The comparison indicates a more polar silica surface for HMS than for SMS and the probe-surface interaction is stronger for HMS than for SMS; in this latter case, lecithin heads and lactose disturb silica polymerization, dependent on the interactions among the various groups. This difference of silica interactions with respect to the two different templating systems is responsible for the different final silica structures for SMS and HMS. To summarize the information provided by CAT16 about the kinetics of formation of SMS and HMS solids, Figure 4 shows the variation of the percentage of the interacting component in the two syntheses. The SMS synthesis seems to follow two different kinetics; up to $t = 100$ min the slope indicates a fast kinetics and the percentage increases from 10 to 70%, then from 100 min to 5 h the increase in the interacting component is much lower (from 70 to 90%) than before. These results may be interpreted either by assuming two different structures formation, or by considering a fast (100 min) solid organization followed by a slow partial restructuration. In both cases, as proposed above, CAT16 is able to monitor the interference of both ethanol and lactose in the silicate network formation and the different interactions occurring in the SMS system where zwitterionic heads and amino groups compete for interacting with the silica surface showing different protonation and bonding equilibria. Further information to clarify the synthesis mechanisms are obtained by using the 5DSA probe, as follows.

EPR Studies of Phospholipids Bilayer Evolution (In Solution) by Progressive Addition of SMS Synthesis Reactants Using 5DSA As Probe. As such as performed for CAT16, the spectra of the solutions containing the reactants of SMS synthesis and 5DSA as a probe were also analyzed by computation of the spectral line shape. Figure S3 (in Supporting Information) shows these computations. The main parameters used for the computations are listed in Table 2. The analysis of these results allowed us to retrieve the following information:

1. First of all, it is useful to underline that the environmental polarity (tested by $\langle A_N \rangle$) of 5DSA is much lower than the polarity for CAT16, since 5DSA is almost water insoluble (the spectrum in pure water is very noisy and poorly informative) and mostly inserts in low polar environments, mainly into lipid aggregates. Consequently, 5DSA monitors structural organization and mobility of the membrane interior, in the lipidic region usually more organized, that is, just below the surfactant heads where the doxyl group is located (Figure 1b). It is known that stearic acid inserted into phospholipid bilayer forms dimers with another stearic acid, and complexes (1:1) with phospholipids by means of electrostatic interactions between carboxylic groups of stearic acids and quaternary ammonium head groups of phospholipids.[41] Consequently, the bilayer becomes more rigid.[42] Also, the bilayer surface tension increases by increasing the stearic acid/phospholipid molar ratio from 0 to 0.3 and leads to an increase of area per lecithin head up to 187 Å^2.[42] Fortunately, EPR only monitors stearic acid/phospholipids interactions, since doxyl groups block the formation of dimers, and in any case the concentration of 5DSA is too low to allow dimer formation. The low amount of probe molecules used in EPR analysis does not influence either the surface tension of the membrane[42] nor its structure. Structure simulation study has shown that fatty acids have their polar heads located below the phosphate groups of the phospholipids and their hydrocarbon chains within the hydrocarbon region of the bilayer (Figure 5).[43] Upon insertion of 5DSA into an ordered bilayer, the EPR spectra computation needs to include as input parameter the order parameter (S), which changes from 0 (no order) to 1 (maximum order). This parameter is therefore introduced in the EPR computation of 5DSA into phospholipid bilayers and/or DDA aggregates and monitors the order of the chains themselves.

2. 5DSA probe monitors the order and packing of the lecithin liposomes in water. 5DSA in lecithin liposomes in water shows a relatively high order parameter ($S = 0.5$), and the mobility and polarity of the probe are quite low ($\tau_{perp} = 1.87$ ns, $\langle A_N \rangle =$ 14.83 G). Such parameters confirm that 5DSA is inserted inside the bilayer with the doxyl probing the hydrocarbon region of the bilayer. In the deprotonated form, the carboxylate group of 5DSA electrostatically interacts with the quaternary ammonium group of lecithin (Figure 5).

3. 5DSA probe monitors the fluidification effect of ethanol in the bilayer. By adding ethanol, as expected by structure simulation,[20] and also monitored by CAT16, the bilayer becomes more fluid; therefore, the order decreases ($S = 0.42$) and the mobility and polarity increase ($\tau_{perp} = 1.76$ ns, $\langle A_N \rangle = 15.00$ G). Ethanol works as a spacer between phospholipid heads giving space to 5DSA, which slightly shifts closer to the lipid heads and feels a higher polarity (Figures 1 and 4).

4. 5DSA probe monitors the perturbation effect of lactose at the membrane intherphase giving rise to a two-components system, one internal and the other external to the bilayer. Again in line with the results from CAT16, the addition of β-lactose

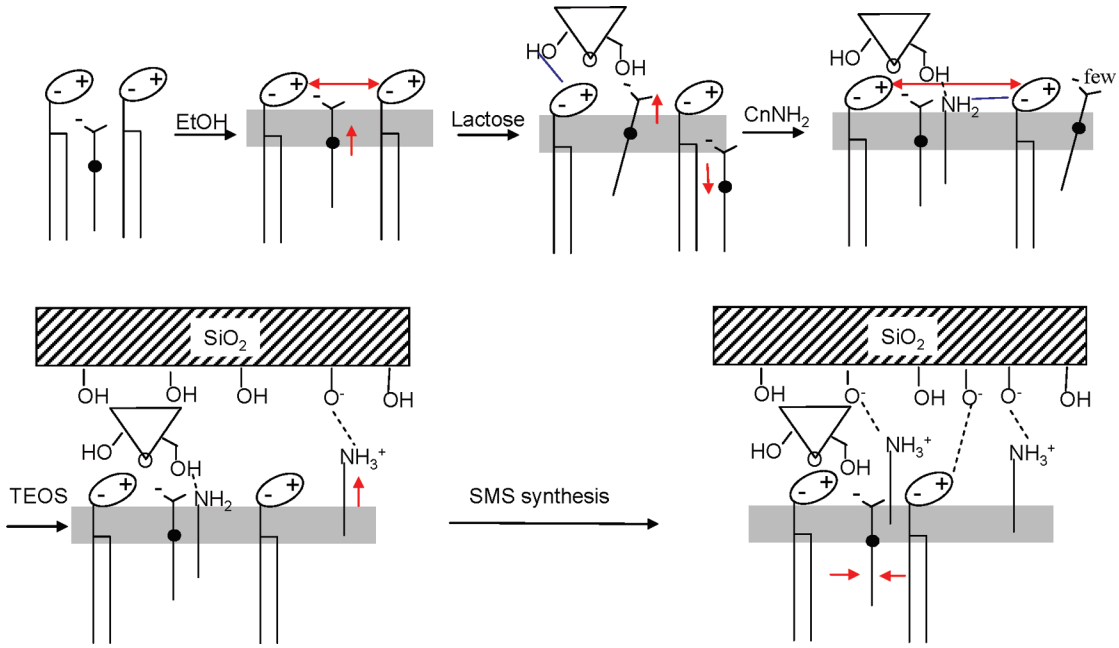

Figure 5. Schematic evolution of the phospholipids bilayer system and 5DSA as a function of progressive addition of SMS reactants. Molecular movements are represented by red arrows. In summary, ethanol works as phospholipid-spacer and induces disordering in the bilayer; β-lactose interacts (by hydrogen-bondings) with the lipid heads; DDA, inserting in the bilayer, impedes lactose−CAT16 hydrogen-bonding and perturbs the bilayer ordering; a poorly structured solid is formed at the beginning of SMS synthesis, which progressively transforms into well-structured SMS due to protonation and consequent electrostatic interactions of DDA amino groups.

TABLE 2: Main Parameters Used for the Computation of 5DSA EPR Spectra (Lec = Lecithin, W = Water, EtOH = Ethanol, Lac = β-Lactose, DDA = Dodecylamine)*

samples- 5DSA	$<A_N>$/G (polarity)	%	τ_{perp}/ns (interaction)	S (order)
Lec−W	14.83	95	1.87	0.5
Lec−W−EtOH	15.00	95	1.76	0.42
Lec−W−EtOH−Lac	14.66	40	1.67	0.38
	15.33	60	0.27	0
Lec−W−EtOH−Lac−DDA	15.00	85	1.59	0.33
		15	0.27	0
Lec−W−EtOH−Lac−DDA−TEOS (begin SMS synthesis)	15.00	95	1.72	0.32
DDA−W	15.00	100	1.05	0.53
DDA−W−EtOH	15.06	100	1.50	0.36
DDA−W−EtOH−TEOS (begin HMS synthesis)	14.50	95	1.25	0

* The g_{ii} components were assumed constant (g_{ii} = 2.009, 2.006, 2.003) and we also assumed $A_{xx} = A_{yy}$= 6 G. $<A_N>$ was calculated as ($A_{xx} + A_{yy} + A_{zz}$)/3. The accuracy of the percent is 1%; the accuracy of $<A_N>$ and τ_{perp} is ± 0.01

significantly disturbs the system. A large fraction (60%) of 5DSA is characterized by a high mobility and polarity (τ_{perp} =0.27 ns, $<A_N>$ = 15.33 G) and a lack of order. As the quaternary ammonium interacts with lactose, 5DSA gains more freedom and moves further to the water/ethanol interphase (Figure 5). On the opposite, 40% of 5DSA remains into the lipid bilayer and is pushed inside the core of the membrane in a less ordered, less polar, and more fluid area of the lipid layer (S = 0.38, τ_{perp} =1.67 ns, $<A_N>$ = 14.66 G). This effect is due to the increase of the interface polarity at the lactose site, where the layer packing is lost and hydrophobic repulsion pushes the low polar probe into the lower polar and more mobile bilayer internal zone. This is also described by simulation results,[20] where an order parameter (named also S) is decreasing along the carbon chain from S = 0.11 at position 3 to S = 0.05 and 0.02 at positions 12 and 16, respectively.

5. 5DSA (in water/EtOH solution) inserts in the DDA/lecithin aggregates that are less ordered than lecithin aggregates. The addition of DDA, as already found by means of CAT16, largely cancels the effect of lactose, and only a 15% fraction of 5DSA remains in the ethanol/water interface. Indeed, 85% of probes is free to interact with phospholipid heads, as in the absence of lactose, since dodecylamine interacts with lactose instead of phospholipid heads (Figure 5). However, the insertion of DDA in the phospholipid structure disturbs 5DSA/lecithin interactions leading to an increase of mobility and decrease of order (τ_{perp} = 1.59 ns, S = 0.33) if compared to 5DSA/lecithin in water/EtOH solution (τ_{perp} =1.76 ns, S = 0.42), while the polarity is the same as in the absence of lactose ($<A_N>$ = 15.00 G). DDA decreased the ordering of the bilayer by inserting between phospholipids and by increasing the area per head. Because of the different locations of the two probes, CAT16 could not monitor such DDA effect while 5DSA did.

6. 5DSA indicates the formation of a bilayer disordered mesophase as templating structure of SMS material (Figure 5). At the beginning of SMS synthesis, after addition of TEOS, the free component almost disappears and migrates into the bilayer and only one component is observed with the same environmental polarity and order as in the absence of TEOS ($<A_N>$ = 15.00 G and S = 0.32). So, the probe monitors a poor variation in the system, that is, a small decrease of the mobility (τ_{perp} =1.72 ns) due to initial solid formation. This shows an

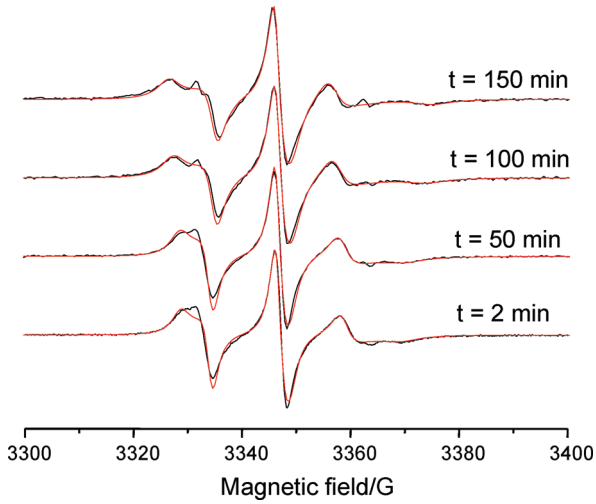

Figure 6. Indicative EPR spectra (experimental, black lines, $T = 310$ K; computed, red lines; magnetic field range, 3300−3400 G) of 5DSA at different synthesis times for the SMS synthesis (lecithin/DDA/lactose/ethanol/water/TEOS).

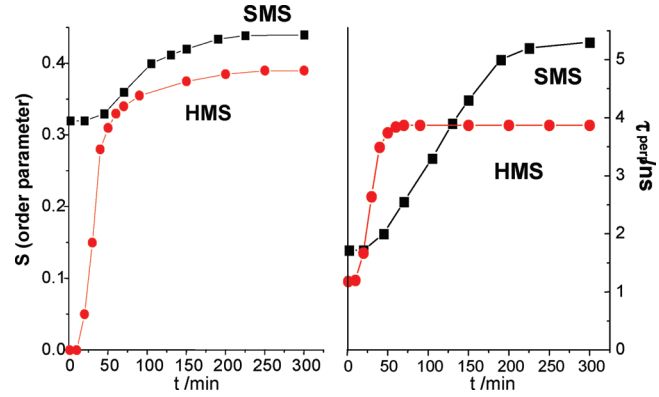

Figure 7. Order parameter (scale from 0 to 0.45) and correlation time for motion (scale from 0 to 5.5 ns) of 5DSA probe as a function of time (scale from 0 to 325 min) for SMS and HMS syntheses. For 5DSA, the percentage of interacting component is constant overtime and equal to 95%.

important point, that the initial templating structure of SMS materials is not a micellar structure, but a bilayer disordered mesophase, unlike HMS material (see below).

EPR Studies of DDA Aggregate Evolution (In Solution) by Progressive Addition of HMS Synthesis Reactants Using 5DSA As Probe. As a comparison, HMS synthesis was also studied using 5DSA probe, and, at first, the effect of the progressive addition of the different reactants was analyzed by computer aided EPR analysis (Figure S4 in Supporting Information).

- 5DSA inserts into the liquid crystal structure of DDA in water. Interestingly, the DDA−water system shows high order, high polarity and low mobility ($S = 0.53$, $\langle A_N \rangle = 15$ G, $\tau_{perp} = 1.05$ ns). This is in line with a nematic liquid crystal organization of DDA in water solution.[44]

- Ethanol promotes 5DSA−DDA interactions and DDA aggregates retain a good chain ordering even at high ethanol content. The addition of ethanol to the DDA−water solution is described in the literature to form a microemulsion,[45] but the perturbation of the DDA structure is lower than expected in such a case; the order decreases, but it is still relatively high ($S = 0.36$), and the mobility of 5DSA probe is lower than in the absence of ethanol, while the polarity increases ($\tau_{perp} = 1.50$ ns, $\langle A_N \rangle = 15.06$ G). As described above, the mobility of CAT16 was higher after addition of ethanol, due to alcohol working as a spacer, penetrating between the DDA heads where also the nitroxide group is positioned and loses the interaction with the amino DDA groups. Conversely, for 5DSA the mobility is decreasing since the doxyl groups (in position 5 on the alkyl chain) goes to interact with the DDA amino groups in a EtOH environment, as confirmed by the increase in polarity around the probe.

- 5DSA indicates that the templating HMS structure is micellar-like. The addition of TEOS, corresponding to the beginning of HMS synthesis, is strongly perturbing the system; the order disappears ($S = 0$), the polarity decreases, and the mobility increases ($\langle A_N \rangle = 14.5$ G, $\tau_{perp} = 1.25$ ns). These data together with the results obtained with CAT16 (showing the solid formation from the beginning of the synthesis) suggests the formation of a silicate network at the DDA micelles surface. This is expected since TEOS hydrolysis induces ionization of DDA amino heads. Because of the repulsing effect of polar-charged silicate surface, the hydrophobic 5DSA is pushed inside the fluid micelle core, where its mobility increases and 5DSA feels the lower polar environment of the hydrophobic tail.

Kinetics of SMS and HMS Synthesis Studied by Means of 5DSA. EPR spectra were recorded over time to monitor SMS (Figure 6) and HMS (Figure S5 in Supporting Information) syntheses by means of 5DSA. In both cases, about 5% of the probes shows fast motion conditions (5% of the probes remains in the ethanol−water solution and is not involved in the solid formation). Therefore, the percentage of what we call "internal component" (probes into the solid-templating aggregates) is constant over time at 95%. The polarity of the internal component remains constant, being $\langle A_N \rangle = 14.5$ and 15.00 G for the HMS and SMS synthesis, respectively; this means that the probe remains in the same environment during solid formation. The doxyl group of 5DSA into SMS is located in a more polar environment than in HMS, since, as discussed above, in the case of HMS synthesis 5DSA is pushed deeper inside the core of the micelles. But, the mobility and order parameters of this "internal component" for both syntheses change over time, as shown in Figure 7. The analysis of the graphs in Figure 7 provides the following information:

- For HMS synthesis, 5DSA monitors that the reorganization of the DDA aggregates continues for about 60 min, while CAT16 monitored no variations in the interactions with the silica groups (silanols and silicates) at the solid interface. Similar discrepancy in the probe responses over time was already found by Zhang et al.[46] due to the different location of the two probes in a CTAB micelles/silica system (for MCM-41 material synthesis); CAT16 monitors the micelle/solid interface, while 5DSA is embedded into the micelles, due to the repulsion caused by the charged silica surface. Therefore, for HMS synthesis the structural variation of the DDA aggregates is finished after 60 min, while the order increased (S from 0 to 0.33) and the mobility decreased (τ_{perp} from 1.25 to 3.0 ns). Similar behavior was previously observed by EPR for MCM-41 synthesis,[23] where 5DSA monitored the elongation of spherical micelles of CTAB, and the formation of an ordered hexagonal structure. In case of HMS, the DDA micelles, formed upon interaction with silica, elongated and ordered to form a defined wormlike aggregate, similar to a disordered hexagonal structure.

- For SMS synthesis, the kinetics monitored by the variation of the order parameter of 5DSA (Figure 5) is similar to the kinetics monitored by the variation of the percentage of interacting component for CAT16 (Figure 3); a faster variation

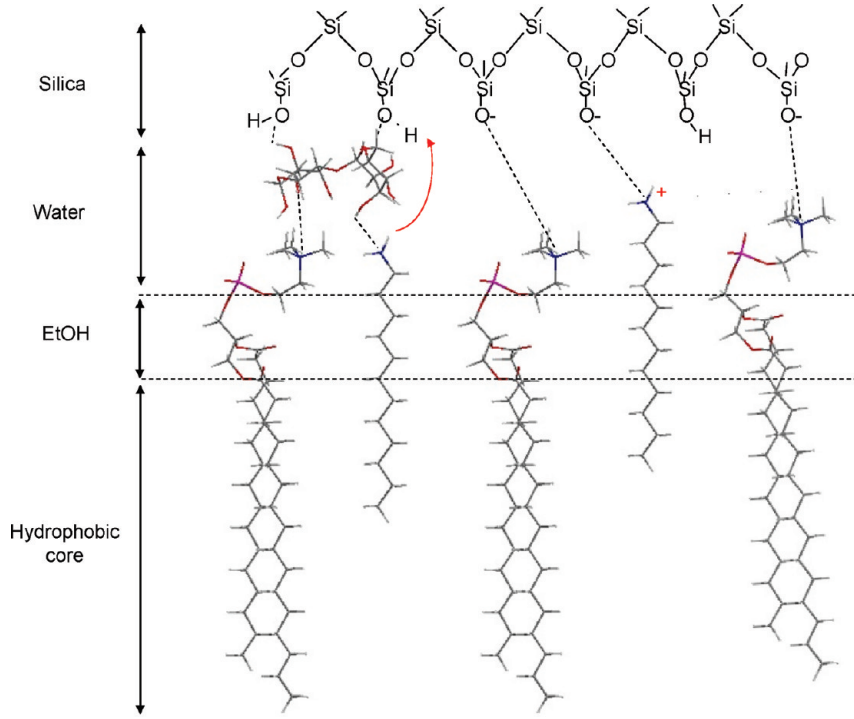

Figure 8. Schematic representation of the interactions between phospholipids, dodecylamine, lactose, and silica inside SMS porous network. Upon SMS formation lactose/dodecylamine interactions are substituted by silica/dodecylammonium interactions, since silanol ionized and dodecylamine protonated.

TABLE 3: Characterization of SMS Materials at Different Synthesis Times: d-Spacing of As-Synthesized and Calcined SMS, Silica Yield, Organic Content, Surface Area, Pore Volume, and Pore Diameter of Calcined SMS

time (min)	Si yield (%)	d_{XRDa} (nm)	d_{XRDc} (nm)	org/SiO_2 (g/g)	S (m^2/g)	V (mL/g)	Dpore (nm)
0	42	6.9	11.3	1.64	418	0.49	5.1
25	61	6.3	6.2	1.57	557	0.78	5.5
70	69	6.6	6.5	1.57	537	0.69	5.4
1440	58	7.0	6.9	1.24	593	0.80	5.9

of the order parameter up to $t = 100$ min and then a slower variation which is finished after almost one day ($S = 0.45$). But with respect to HMS, the variation of S is much smaller, since the starting aggregates are already partially ordered at the beginning of the synthesis. This confirms that the starting material is not a micellar solution, but an interconnected bilayer structure, which is responsible to produce the solid sponge material. Also the mobility of 5DSA at the end of the synthesis is lower for SMS ($\tau_{perp} = 5.30$ ns) than for HMS ($\tau_{perp} = 3.00$ ns) since the aggregates into SMS are well packed (more than into HMS), and the probe interacts with the phospholipids. The increasing packing of phospholipids induces a decrease in rotational mobility and an increase of the chain order felt by 5DSA.

EPR experiments allowed us to propose different kinds of interactions occurring inside the SMS materials. To draw a more realistic qualitative interactions scheme (Figure 8), we calculated Mulliken atomic charges for the different molecules, dipalmitoyl phosphatidylcholine, β-lactose, dodecylamine, and dodecylammonium. Details about calculations, molecular structures, and charges are presented in Figure S6 and Table S1, respectively, in Supporting Information.

Solid-State Characterization during SMS Synthesis. To better identify the templating phase, different SMS materials were prepared at different reaction times and the resulting solids were characterized by XRD, nitrogen adsorption, SEM, and TEM. The main results are listed in Table 3. The SMS composition (~1.5 g organics per g of silica) is slightly changing over time except in the first 25 min where the silica yield is increasing from 40 to 60% confirming the higher silica condensation during this time. XRD pattern (Figure 9) of SMS samples prepared at different synthesis time shows that SMS material is already present at time 0 of the synthesis, that is, after 15 min stirring with TEOS ($t = 0$ min in static) with a diffraction peak at 6.9 nm. The lack of overdiffraction peaks did not allow us to evaluate the real distance between pores, since wall thickness needs to be included. This XRD peak mainly reveals a repeating distance in the porosity. The peak does not change position over time. This indicates that the material is formed at the beginning of the synthesis. Furthermore, the solid chemical structure becomes more organized as tested by the increase in XRD peak intensity (due to an increased electron density). This result is in perfect agreement with the results by EPR. On the other hand, SEM images (Figure 10a) show that spherical particles are formed since the beginning of the synthesis and enlarge within time from 500 nm to 2 μm, as expected for better organized solid particles. Upon calcination the materials are stable, as a similar diffraction peak is observed at around 6.5 nm. This means that the structure is tridimensional and not lamellar since it does not collapse after calcination. This is also revealed by TEM (Figure 10b), which shows a mesoporous spongelike structure for all synthesis time with pore size in the range of 5−7 nm. On this basis, the porous network may be represented schematically as in Figure 10c with cages of 7 nm and connecting channels of 5 nm in line with a templating structure constituted by interconnected bilayers of phospholipids.

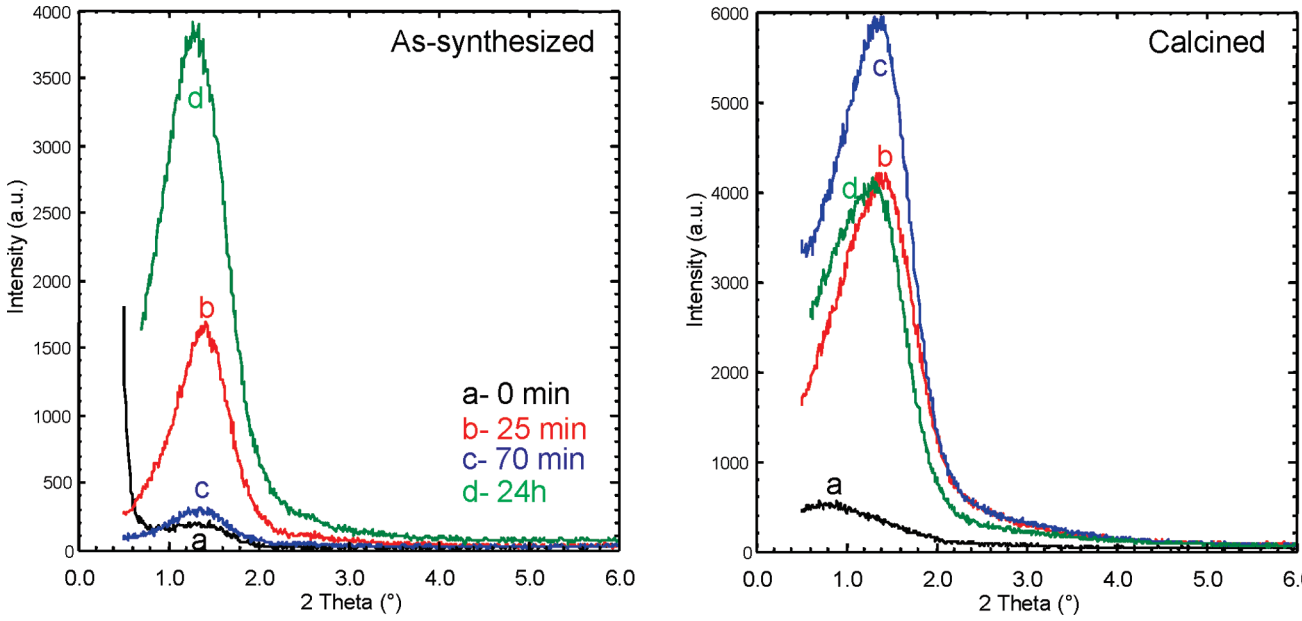

Figure 9. XRD of as-synthesized and calcined SMS at various synthesis times: intensity (arbitrary units, from 0 to 4000 for as-synthesized material; from 0 to 6000 for calcined material) as a function of 2θ angle (scale from 0 to 6°).

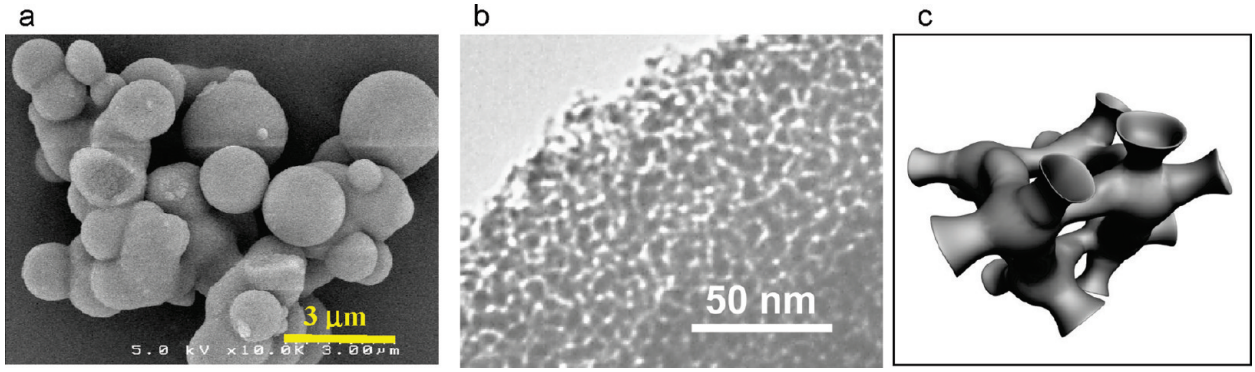

Figure 10. (a) SEM and (b) TEM of SMS materials; (c) schematic representation of the pore structure, corresponding to the disordered phospholipid bilayer structure templating SMS materials.

The pore network of SMS was also analyzed by nitrogen sorption on calcined materials (Figure 11) and reveals a constant-overtime pore size of about 5.5 nm. The slight delay in desorption observed in the nitrogen isotherm indicates that the mesopores feature slight constrictions. On this basis, we estimate a cavity size of 6.5 nm with constriction of about 4.5 nm.[47] This pore size is in accordance with the values measured in TEM images and with the size of a lecithin bilayer (5.0 nm for dehydrated bilayer and 6.5 nm for fully hydrated bilayer).[48] Since no evolution in the porosity is noticed within time, we assume that the disordered phospholipid bilayer formed in the solution before adding TEOS has the same structure as the porosity of SMS material. This means that the template mesostructure for SMS synthesis is isotropic 3D, similar to a disordered bicontinuous gyroid structure. During synthesis time, the pore volume and the surface area of SMS are increasing (Figure 11, Table 3), due to redistribution of silica inside the network. This leads to thin walls between pores at longer synthesis time. In the first minutes of synthesis, most silica is under noncondensed silanol form and only few silicates electrostatically interact with phospholipids heads. We suppose that these noncondensed silanols migrate along the water/silica network to interact with "free" (noninteracting with lactose) phospholipids heads. Therefore, these silanols take part to the exchange of interactions between dodecylamine/lactose and

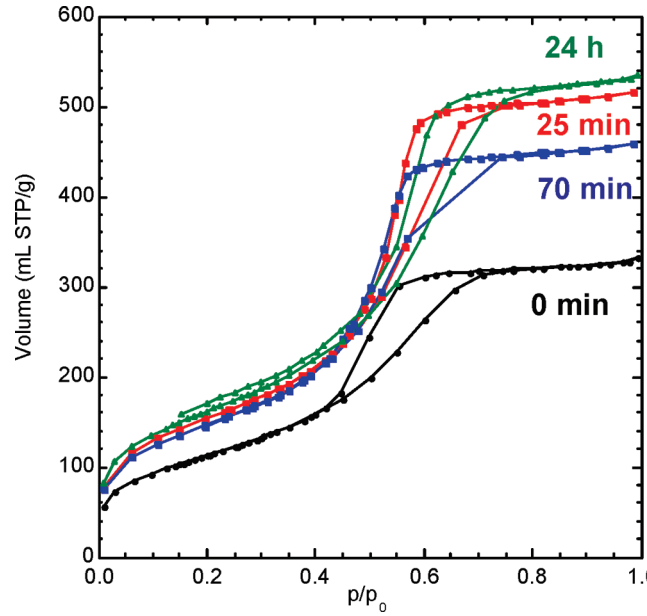

Figure 11. Nitrogen sorption isotherm at 77 K of calcined SMS materials at various synthesis times. The volume (scale from 0 to 600 mL STP/g) is plotted as a function of pressure ratio p/p_0 (scale from 0 to 1).

TABLE 4: Porosity Characterization of SMS Materials Compared to HMS, MCM-41, MCM-48: Total Surface Area by BET (S_{BET}), Pore Volume (V), Pore Diameter by BdB Equation from Desorption Isotherm (D_{BdB}) and by Gurvitch Equation ($4V/S^*$), Shape Factor α (α = 1, Lamellar; α = 2, Cylindrical; α = 3, Spherical)[a]

materials	S_{BET} m²/g	C_{BET}	V mL/g	D_{BdB} nm	$4\ V/S^*$> nm	$\alpha = D_{BdB}/(2\ V/S^*)$
SMS	593	86	0.78	5.74	6.08	1.89
HMS	931	61	0.77	3.51	4.07	1.72
MCM-41	825	80	0.72	4.11	4.12	2.00
MCM-48	1086	75	0.94	3.72	3.99	1.87

[a] The surface of nitrogen molecule for mild hydrophilic sample as the one studied (C_{BET} = 70−80) has been assumed to be 14.5 Å² instead of 16.2 Å², classically used in BET equation. The mesoporous surface S and the pore diameter $4V/S^*$ were then recalculated considering $S^* = S$ (14.5/16.2).

dodecylamine/silica by protonating DDA, as suggested by EPR results (Figure 8). As a consequence, the silica condensation leads to thinner pore walls. By combination with EPR results on 5DSA, we propose that this migration has the further effects to elongate the pore channels to approach the phospholipids heads to each other and therefore to increase the order in the phospholipid bilayer embedded into silica.

It is noteworthy that a difference exists between the pore diameter determined from BdB method using the desorption pressure of nitrogen isotherm, and the diameter obtained by means of geometrical $4\ V/S^*$ method, used for independent cylindrical pores. This difference is evidenced from the shape of the pores differing from the cylindrical geometry by the existence of negative curvature, due to cavities and/or connections between channels. Negative pore curvatures feature less energetic surfaces and are less favorable for nitrogen adsorption, which contributes to a decrease in the S/V ratio of the material.[49] It has already been noticed that the existence of connections or constrictions into pores delays the adsorption and leads to a less vertical adsorption.[47] This is observed for SMS material and also for HMS compared to MCM-41. To evaluate the degree of negative curvature existing in the materials, we proposed to use a shape factor α, closely related to the shape factor described in the Kelvin equation,[49] correlating the pore diameter obtained from desorption pressure of the isotherm (D_{BdB}) to the geometric pore evaluation $2\alpha V/S^*$

$$\alpha = D_{Bdb}/(2V/S^*)$$

In Kelvin equation, the shape factor α is equal to 1 for a lamellar surface, to 2 for a cylinder, and to 3 for a sphere.[49] Simulated experiments have provided the shape factor for MCM-48 (cubic structure with gyroid surface) between 1.7 and 1.9,[49] depending on its wall-thickness from 0 to 1.2 nm. In Table 4, the shape factor of final SMS and HMS materials were compared with the ones for homemade MCM-41 (hexagonal structure) and MCM-48 materials.. We calculated values of 2.00 and 1.87 for MCM-41 and MCM-48, respectively, in accordance with theoretical values for a hexagonal and a gyroid structure. For SMS, we have found α = 1.89, close to the one obtained for MCM-48, in agreement with the existence of a bicontinuous disordered gyroid phospholipid bilayer structure as template for SMS materials. For HMS materials, the shape factor is surprisingly very low with a value of 1.72, whereas a cylindrical shape of pore is expected (α = 2). This high degree of negative curvature likely comes from undulations in the pore of HMS materials with a wormlike structure.

Conclusion

A comparative EPR analysis of SMS and HMS synthesis mixtures provided information on the effect of different reactants on the phospholipids bilayer. Ethanol inserts among the head groups of phospholipids and/or dodecylamine, giving rise to undulations (wave effect) in the lipid bilayer structure. Lactose is located at the water/membrane interface and interacts through hydrogen bonding with the lipid heads. Adding a silica source to the "undulated" mesophase does not change its structure. Then, the mechanism of SMS formation was elucidated by means of a combined EPR and solid characterization study. The new mesophase of phospholipids, formed by the addition of ethanol and dodecylamine, gave rise, by silica condensation, to a disordered isotropic cubic lipid phase with a gyroid-type surface, never observed before. Silica condensation also allows the bilayer to increase its packing, leading to a slight elongation of the channels. Further, EPR, XRD, and nitrogen adsorption analyses over the synthesis time indicated that the kinetics of formation of SMS materials is slow (4 h) due to a progressive migration of silicates along the cubic mesophase of phospholipids. Conversely, a polar HMS solid, templated by dodecylamine and ethanol, forms in few minutes (<1 h), transforming dodecylamine/silicate micelles into a wormlike structure with undulated channels. SEM and TEM images also showed the growing size of spherical particles with a sponge mesoporous structure.

This study further demonstrated the power of combining in situ experiments by means of EPR probes inserted in surfactant/silica system with solid state characterization to understand materials formation and to elucidate the templating mesophase.

Acknowledgment. The authors thank Christine Biolley for her help in the synthesis.

Supporting Information Available: Figures S1−S5. Experimental (310 K) and computed EPR spectra of CAT16 and 5DSA in water, lecithin/water, lecithin/water/ethanol, lecithin/water/ethanol/lactose, lecithin/water/ethanol/lactose/dodecylamine, lecithin/water/ethanol /lactose/dodecylamine/TEOS (beginning of SMS synthesis), dodecylamine/water, dodecylamine/water/ethanol, dodecylamine/water/ethanol/TEOS (beginning of HMS synthesis and various synthesis times). Figure S6. Structures of dipalmitoyl phosphatidylcholine; β-lactose; protonated dodecylamine and dodecylamine with the indications of the atoms for which atomic charges were calculated. The atomic charges of the indicated atoms in these four molecules are listed in Table S1. This material is available free of charge via the Internet at http://pubs.acs.org.

References and Notes

(1) (a) Chiola, V.; Ritsko, J. E.; Vanderpool, C. D. U.S. Patent 3,556,725, 1971. (b) DiRenzo, F.; Cambon, H.; Dutartre, R. *Microporous Mater.* **1997**, *10*, 283.

(2) Beck, J. S.; Vartuli, J. C.; Roth, W. J.; Leonowicz, M. E.; Kresge, C. T.; Schmidt, K. D.; Chu, C. T. W.; Olson, D. H.; Sheppard, E. W.; McCullen, S. B.; Higgins, J. B.; Schlenker, J. L. *J. Am. Chem. Soc.* **1992**, *114*, 10834.

(3) Di Renzo, F.; Galarneau, A.; Trens, P.; Fajula, F. *Handbook of porous materials*; Schüth, F., Sing, K., Weitkamp, J., Eds.;Wiley-VCH, New York, 2002; p 1311.
(4) Kim, J.; Grate, J. W.; Wang, P. *Chem. Eng. Sci.* **2005**, *61*, 1017.
(5) Hartmann, M. *Chem. Mater.* **2005**, *17*, 4577.
(6) Dai, Z.; Xu, X.; Wu, L.; Ju, H. *Electroanalysis* **2005**, *17*, 1571.
(7) Munoz, B.; Ramila, A.; Perez Pariente, J.; Diaz, I.; Vallet Regi, M. *Chem. Mater.* **2003**, *15*, 500.
(8) Brennan, J. D.; Benjamin, D.; DiBattista, E.; Gulcev, M. D. *Chem. Mater.* **2003**, *15*, 737.
(9) Nassif, N.; Roux, C.; Coradin, T.; Rager, M. N.; Bouvet, O. M. M.; Livage, J. *J. Mater. Chem.* **2003**, *13*, 203.
(10) Nassif, N.; Bouvet, O.; Rager, M. N.; Roux, C.; Coradin, T.; Livage, J. *Nat. Mater.* **2002**, *1*, 42.
(11) Nassif, N.; Coiffier, A.; Coradin, T.; Roux, C.; Livage, J.; Bouvet, O. *J. Sol.-Gel. Sci. Technol.* **2003**, *26*, 1141.
(12) Reetz, M. T. *Tetrahedron* **2002**, *58*, 6595.
(13) Reetz, M. T.; Tielmann, P.; Wiesenhofer, W.; Konen, W.; Zonta, A. *Adv. Synth. Catal.* **2003**, *345*, 717.
(14) Mureseanu, M.; Galarneau, A.; Renard, G.; Fajula, F. *Langmuir* **2005**, *21*, 4648.
(15) Galarneau, A.; Mureseanu, M.; Atger, S.; Renard, G.; Fajula, F. *New J. Chem.* **2006**, *30*, 562.
(16) Galarneau, A.; Renard, G.; Fajula, F. patent, Fr. 04.13119, 2006.
(17) Wendel, A. *Kirk-Othmer Encycl. Chem. Technol.* **1995**, *15*, 192.
(18) Williams, A. C.; Barry, B. W. *Adv. Drug Deliver. Rev.* **2004**, *56*, 603.
(19) Kurihara-Bergstrom, T.; Knutson, K.; De Noble, L. J.; Goates, C. Y. *Pharm. Res.* **1990**, *7*, 762.
(20) Gurtovenko, A. A.; Anwar, J. *J. Phys. Chem. B* **2009**, *113*, 1983.
(21) Holte, L. L.; Gawrish, K. *Biochemistry* **1997**, *36*, 4669.
(22) Mou, J.; Yang, J.; Huang, C.; Shao, Z. *Biochemistry* **1994**, *33*, 9981.
(23) Galarneau, A.; Di Renzo, F.; Fajula, F.; Mollo, L.; Fubini, B.; Ottaviani, M. F. *J. Colloid Interface Sci.* **1998**, *201*, 105.
(24) Ottaviani, M. F.; Galarneau, A.; Desplantier-Giscard, D.; Di Renzo, F.; Fajula, F. *Microporous Mesoporous Mater.* **2001**, *44*−*45*, 1.
(25) Ottaviani, M. F.; Moscatelli, A.; Desplantier-Giscard, D.; Di Renzo, F.; Kooyman, P. J.; Alonso, B.; Galarneau, A. *J. Phys. Chem. B* **2004**, *108*, 12123.
(26) Galarneau, A.; Cangiotti, M.; Di Renzo, F.; Fajula, F.; Ottaviani, M. F. *J. Phys. Chem. B* **2006**, *110*, 4058.
(27) Galarneau, A.; Cangiott i, M.; Di Renzo, F.; Sartori, F.; Ottaviani, M. F. *J. Phys. Chem. B* **2006**, *110*, 20202.
(28) Zhang, J.; Luz, Z; Goldfarb, D. *J. Phys. Chem. B* **1997**, *101*, 7087.
(29) Zhang, J; Luz, Z; Zimmermann, H; Goldfarb, D. *J. Phys. Chem. B* **2000**, *104*, 279.
(30) Ruthstein, S; Schmidt, J; Kesselman, E; Talmon, Y.; Goldfarb, D. *J. Am. Chem. Soc.* **2006**, *128*, 3366.
(31) Ruthstein, S; Frydman, V; Goldfarb, D. *J. Phys. Chem. B* **2004**, *108*, 9016.
(32) Ruthstein, S; Goldfarb, D. *J. Phys. Chem. C* **2008**, *112*, 7102.
(33) Tanev, P. T.; Pinnavaia, T. J. *Science* **1995**, *267*, 865.
(34) Zhang, W. Z.; Pauly, T. R.; Pinnavaia, T. J. *Chem. Mater.* **1997**, *9*, 2491.
(35) DiRenzo, F.; Testa, F.; Chen, J. D.; Cambon, H.; Galarneau, A.; Plee, D.; Fajula, F. *Microporous Mesoporous Mater.* **1999**, *28*, 437.
(36) Galarneau, A.; Renard, G.; Mureseanu, M.; Tourrette, A.; Biolley, C.; Choi, M.; Ryoo, R.; Di Renzo, F.; Fajula, F. *Microporous Mesoporous Mater.* **2007**, *104*, 103.
(37) Schneider, D. J.; Freed, J. H. In *Biological Magnetic Resonance. Spin Labeling. Theory and Applications*; Berliner, L. J.; Reuben, J., Eds.; Plenum Press: New York, 1989; Vol. *8*, p 1.
(38) Budil, D. E.; Lee, S.; Saxena, S.; Freed, J. H. *J. Magn. Res. A* **1996**, *120*, 155.
(39) Broekhoff, J. C. P.; Boer, J. H.d. *J. Catal.* **1968**, *10*, 377.
(40) Galarneau, A.; Desplantier, D.; Dutartre, R.; DiRenzo, F. *Microporous Mesoporous Mater.* **1999**, *27*, 297.
(41) Petelska, A. D.; Naumovwicz, M.; Figaszewski, Z. A. *Bioelectrochemistry* **2007**, *70*, 28.
(42) Inoue, T.; Yanagihara, S.; Misono, Y.; Suzuki, M. *Chem. Phys. Lipids* **2001**, *109*, 117.
(43) Notman, R.; Noro, M. G.; Anwar, J. *J. Phys. Chem. B* **2007**, *111*, 12748.
(44) Ralston, A. W.; Hoerr, C. W.; Hoffman, E. J. *J. Am. Chem. Soc.* **1942**, *64*, 1516.
(45) Caldararu, H.; Caragheorgheopol, A.; Savonea, F; Macquarrie, D. J.; Gilbert, B. C. *J. Phys Chem. B* **2003**, *107*, 6032.
(46) Zhang, J.; Carl, P. J.; Zimmermann, H.; Goldfarb, D. *J. Phys. Chem. B* **2002**, *106*, 5382.
(47) Coasne, B.; Galarneau, A.; Di Renzo, F.; Pellenq, R. J. M. *J. Phys. Chem. C* **2007**, *111*, 15759.
(48) Small, D. *J. Lipid Res.* **1967**, 8.
(49) Coasne, B.; Galarneau, A.; Di Renzo, F.; Pellenq, R. J. M. *Langmuir* **2006**, *111*, 11097.

JP908828Q